INFECTION AND IMMUNITY, Aug. 1999, p. 4171–4182 Vol. 67, No. 8
0019-9567/99/$04.00+0

Campylobacter jejuni 81-176 Associates with Microtubules and Dynein during Invasion of Human Intestinal Cells

LAN HU AND DENNIS J. KOPECKO*

Laboratory of Enteric and Sexually Transmitted Diseases, Center for Biologics Evaluation and Research, Food and Drug Administration. Bethesda, Maryland 20892

Received 14 January 1999/Returned for modification 25 March 1999/Accepted 4 May 1999

Campylobacter jejuni **uptake into cultured INT407 cells was analyzed kinetically over a wide range of starting multiplicities of infection (MOI; from 0.02 to 20,000 bacteria/epithelial cell). The efficiency of internalization was the highest at MOI of 0.02 and decreased steadily at higher MOIs, presumably due to reported *C. jejuni* autoagglutination at higher densities. Total internalized *Campylobacter* CFU increased gradually from an MOI of 0.02 to a peak at an MOI of 200 (reaching an average of two bacteria internalized per epithelial cell) and decreased at higher MOIs. The invasion process was apparently saturated within 2 h at an MOI of 200, indicating stringent host cell limitations on this entry process. Furthermore, whereas control *Salmonella typhi* invaded all monolayer cells within 1 h, only two-thirds of monolayer cells were infected after 2 h with *C. jejuni* at MOIs of 200 to 2,000. The percentage of *Campylobacter*-infected host cells gradually increased to 85% after 7 h of infection, suggesting that *C. jejuni* entry may be host cell cycle dependent. Direct evidence of the involvement of microtubules in *C. jejuni* internalization, suggested previously by biochemical inhibitor studies, was obtained by time course immunofluorescence microscopic analyses. Bacteria initially bound to the tips of host cell membrane extensions containing microtubules, then aligned in parallel with microtubules during entry, colocalized specifically with microtubules and dynein but not with microfilaments, and moved over 4 h, presumably via microtubules to the perinuclear region of host cells. Orthovanadate, which inhibits dynein activity, specifically reduced *C. jejuni* 81-176 entry, suggesting that this molecular motor is involved in entry and endosome trafficking during this novel bacterial internalization process. Collectively, these data suggest that *C. jejuni* enters host cells in a targeted and tightly controlled process leading to uptake into an endosomal vacuole which apparently moves intracellularly along microtubules via the molecular motor, dynein, to the perinuclear region.**

Campylobacter jejuni and *C. coli* are among the most common causes of human diarrheal diseases and are estimated to cause illness annually in 1% of the U.S. population (4, 59, 60). These *Campylobacter* spp. are spiral, gram-negative, polarly flagellated, and strictly microaerophilic bacteria, a diagnostic requisite that both delayed their recognition as human pathogens and likely hampers accurate measure of their true incidence today. The pathophysiology of diarrheal disease caused by *Campylobacter* spp. is poorly understood, although as few as 5 to 500 organisms given orally can cause human diarrheal illness (1, 54). Clinical symptoms range from a protracted watery diarrhea to bloody diarrhea with fever, abdominal cramps, and the presence of fecal leukocytes (1, 2, 4, 12). In addition, recent evidence has revealed several *C. jejuni* serotypes as the causative factors of postdiarrheal Guillain-Barré paralysis (3), amplifying the importance of this pathogen. The results of intestinal biopsies of patients, infected primates, and several other experimental model animals have demonstrated the ability of *C. jejuni* to invade enterocytes and suggest that some *Campylobacter* spp. cause invasive intestinal disease (2).

The cultured eukaryotic cell invasion assay technique (13) has become a standard experimental procedure in the study of bacterial internalization mechanisms. Bacterial internalization has typically been observed to involve rearrangement of the host cytoskeletal structure, resulting in endocytosis of the pathogen. The cytoskeleton of eukaryotic cells is a complex array of proteins, the most prominent of which are actin and tubulin, which comprise microfilaments (MFs) and microtubules (MTs), respectively. These filamentous structures, together with intermediate filaments, are involved in both cellular and subcellular movements and in the determination of host cell shape. Most invasive enteric organisms (e.g., *Salmonella*, *Shigella*, *Listeria*, and *Yersinia* spp. [7, 16, 18, 31, 43]) have been found to trigger largely MF-dependent entry pathways.

The ability of *C. jejuni* to invade cultured human intestinal epithelial cells has been found to be strain dependent and quite variable in efficiency (10, 15, 33, 37, 48). *Campylobacter* internalization has been variously reported to require MFs (15, 36), MTs (48), both MFs and MTs (48), or neither (55), depending on the host cell type and methods used and the *C. jejuni* strain studied. Only a few *C. jejuni* strains have been studied in any detail for invasion mechanism, leaving the host cell cytoskeletal requirements for and the mechanism(s) of *Campylobacter* entry into epithelial cells an open question. To confuse matters more, some *C. jejuni* isolates have been associated with diarrhea and others have been associated with dysentery; it is not known whether only some strains cause invasive disease. In 1993, Oelschlaeger et al. (48) described a relatively high efficiency invasion process for *C. jejuni* 81-176, a well-studied strain which has been shown to cause disease by human feeding (1), and demonstrated through the use of biochemical inhibitors that *C. jejuni* 81-176 enters cultured human intestinal INT407 cells via a novel process that requires polymerized MTs, but not MFs as required by *Salmonella typhi* for entry.

The present study was undertaken specifically to better characterize the *C. jejuni* 81-176 invasion mechanism through (i) kinetic analyses of *C. jejuni* 81-176 invasion to ascertain the effects of time and bacterial concentration on maximal invasion

* Corresponding author. Mailing address: Laboratory of Enteric and Sexually Transmitted Diseases, FDA-Center for Biologics Evaluation and Research, Bldg. 29/420, NIH Campus, Bethesda, MD 20892. Phone: (301) 496-1893. Fax: (301) 402-2776. E-mail: Kopecko@cber.fda.gov.

and the percentage of host cells infected, (ii) two-dimensional and laser scanning confocal immunofluorescence microscopic analyses and biochemical inhibition studies to characterize further the involvement of MTs in the invasion process; and (iii) assessment of the potential role of the minus-end-directed MT motor protein dynein in the *C. jejuni* invasion mechanism.

MATERIALS AND METHODS

Bacterial strains, cell lines, media, and culture conditions. *C. jejuni* 81-176, an often-studied strain obtained originally from the stool of a colitis patient (38), and strain RY213, a noninvasive mutant of *C. jejuni* 81-176 with two copies of the *cheY* gene (64), were grown in Mueller-Hinton (M-H) biphasic medium and on M-H agar (Difco) under a *Campylobacter* microaerophilic atmosphere of 10% O_2–5% CO_2–85% N_2. Experimental control bacteria, invasive *S. typhi* Ty2W and noninvasive *Escherichia coli* HB101, were grown at 37°C in L broth (Difco) to mid-log phase for invasion studies. Human embryonic intestinal epithelial (INT407) and human colon cancer (Caco-2) cells, obtained from the American Type Culture Collection, were maintained in liquid nitrogen and cultivated in minimal essential media with 10% heat-inactivated fetal calf serum (Gibco), 0.2 mM L-glutamine, and 0.1 mM nonessential amino acids, as recommended by the American Type Culture Collection. Media for Caco-2 cells also contained 1 mM sodium pyruvate.

Invasion assay. The assay was performed essentially as described previously (14, 48) except that the bacterial inoculum was not centrifuged to initiate contact with epithelial cells and monolayer cells were not completely confluent. Monolayer cells were split and grown for 24 h before use in invasion assays. To a ~80% confluent monolayer of about 10^5 epithelial cells per well of a 24-well plate, different multiplicities of infection (MOIs) of mid-log-phase (optical density at 600 nm [OD_{600}] of 0.6 to 0.8) bacteria were added in 50 μl of minimal essential medium to 1 ml of culture medium per well. Infected monolayers were typically incubated for 2 h at 37°C in a 5% CO_2–95% air atmosphere to allow invasion to occur. For time course analyses, the invasion period was varied from 0 to 120 min and in some studies up to 7 h. Following this invasion period, the monolayer was washed three times with Earle's balanced salt solution with Ca^{2+} and Mg^{2+} (EBSS) (Gibco) and incubated for another 2 h in fresh tissue culture medium containing gentamicin (100 μg/ml) to kill extracellular bacteria. After the gentamicin kill period, the infected monolayers were washed as described above and lysed with 0.1% Triton X-100 in phosphate-buffered saline (PBS) for 15 min at room temperature on an orbital shaker. Following serial dilution in PBS, released intracellular bacteria were enumerated by colony count on M-H agar cultured under *Campylobacter* atmospheric conditions. Each internalization assay was performed simultaneously in three separate wells and repeated on at least three separate occasions. Results are presented as the mean ± standard error (SE). Control studies were conducted to verify that a 1-h exposure of *C. jejuni* to 100 μg of gentamicin per ml resulted in 100% kill. Also, trypan blue assays verified that no increased death of cultured cells occurred over the time course of these studies at various starting MOIs. Certain invasion levels were compared by the Student *t* test for statistically significant differences.

Invasion assays in the presence of biochemical inhibitors. Inhibitors of eukaryotic cell processes were generally added to the monolayer 1 h prior to the addition of bacteria and were maintained throughout the 2-h invasion period, as described previously (48). Bacteria were typically added at an MOI of 20 for these inhibitor studies. Note that the relative degree of inhibition was not affected by varying the MOI from 2 to 2,000. The dynein inhibitor sodium orthovanadate (22) was added to host cells 30 min prior to the addition of bacteria and was maintained throughout the invasion period. Then the infected monolayer was washed three times with EBSS and incubated for another 2 h in fresh culture medium containing gentamicin (100 μg/ml) to kill extracellular bacteria. Subsequently, the infected monolayers were washed and internalized bacteria were enumerated by plate count as described above. Control studies were conducted to verify that at the concentrations used each inhibitor did not affect epithelial cell viability over the assay period, as measured by trypan blue staining, or bacterial viability, as assessed by viable plate count. *S. typhi* was used here as a MF-dependent invasion control. All invasion inhibition assays were conducted in three separate wells during each assay and were repeated on three separate occasions.

Direct visualization of internalized bacteria by the AO-CV method. Infected monolayers, grown on glass coverslips placed in 24-well tissue culture plates, were stained at various times postinfection with 0.01% acridine orange (AO) in Gey's solution for 45 s, rinsed in EBSS, counterstained with 0.5% crystal violet (CV) in 0.15% NaCl for another 45 s, and then washed with EBSS (29, 44). Glass coverslips with stained preparations were mounted on slides and were viewed with a fluorescence microscope. Under these conditions, intracellular viable bacteria appeared green, nonviable bacteria appeared orange, and all extracellular bacteria counterstained a dark violet. Manual, multiplanar focusing was used to visualize and enumerate all bacteria present in each three-dimensional host cell. The percentage of infected host cells at each time point was extrapolated by assessing the presence or absence of bacteria in at least 30 host cells in several different microscopic fields.

Indirect immunofluorescence assays. Intestinal cells were grown as described above on coverslips for 24 h. INT407 cells were infected with *C. jejuni* 81-176 at an MOI of 20 for 0.5, 1, 2, or 4 h at 37°C. The monolayer cells were washed three times, fixed, and permeabilized by the method of Osborn and Weber (49). In brief, samples were washed three times with PBS, fixed at room temperature with 3.7% paraformaldehyde for 15 min, incubated with 1% glycine in PBS to quench excess aldehyde groups, permeabilized with 0.1% Triton X-100 for 5 min, and treated with 1% bovine serum albumin in PBS for 15 min to reduce nonspecific binding of added antibodies. Thereafter, the monolayer was incubated at 37°C for 1 h with mouse monoclonal anti-α-tubulin antibody (Sigma catalog no. T9026) diluted 1:50 in PBS and rabbit polyclonal anti-*C. jejuni* 81-176 antibody (1631; kindly provided by P. Guerry-Kopecko) diluted 1:4,000 in PBS or *Salmonella* group D antiserum (Difco) diluted 1:100. Treated monolayers were washed three times for 10 min each with PBS and incubated for 1 h with Texas red-X-conjugated goat anti-mouse immunoglobulin G and with fluorescein isothiocyanate (FITC)- or Oregon Green 514-conjugated goat anti-rabbit immunoglobulin G (Molecular Probes or Sigma). In some studies, the fluorescent stains were reversed. To stain actin-containing structures, the host cells were treated with coumarin phenyl isothiocyanate-labeled phalloidin (Sigma) for 30 min at 37°C. Host cell dynein was examined by using a mouse monoclonal antidynein antibody (Sigma catalog no. D5167). Each stained monolayer was mounted with Vectashield mounting medium to reduce photobleaching and was viewed with a Zeiss MC100 fluorescence microscope and a Bio-Rad MRC600 confocal laser scanning microscope. Antibody specificities were verified in control studies with noninfected and infected host cells, before and after reaction with primary antibody or secondary antibody.

The finger-like, MT-based membrane extensions shown in Fig. 3A and 4A were not observed with light immunostaining but instead required dense immunostaining of MTs. Adobe Photoshop was used on computer-scanned images of the above-described immunofluorescence micrographs to deintensify the staining of the cell body while maintaining the intensity of MT staining at the cellular margins, which resulted in enhanced visualization of these thin MT-based membrane protrusions.

RESULTS

Bacterial concentration and growth phase dependence for optimal *C. jejuni* internalization. INT407 cells were infected with different starting MOIs (number of bacteria added per epithelial cell) of mid-log-phase *C. jejuni* 81-176 and incubated for 2 h (the invasion period) and then for another 2 h in the presence of gentamicin (the gentamicin kill period) prior to enumeration of internalized bacteria. The highest invasion efficiency (3.5%) was observed at the lowest MOI of 0.02, and invasion efficiency decreased steadily at higher MOIs (Fig. 1A). This observation contrasts sharply with our published kinetic analyses of *S. typhi* invasion, where the invasion efficiency was suboptimal at lower MOIs, reached a broad optimum at an MOI of ~40, and decreased markedly at higher bacterial concentrations (29). On the other hand, the total number of internalized bacteria increased with greater bacterial concentrations from an MOI of 0.02 steadily to a broad maximal peak at an MOI of 200 and decreased thereafter (Fig. 1B). At an MOI of 200, approximately two bacteria were internalized per epithelial cell (average for all host cells) (Fig. 1C). In limited studies, early-stationary-phase (OD_{600} of 1.2) *C. jejuni* 81-176 organisms added at the optimal MOI of 200 were reduced about three- to fivefold in typical invasion efficiency relative to mid-log-phase bacteria.

For an experimental control, the noninvasive *E. coli* strain HB101 was internalized at a ≥1,000-fold-lower level at an MOI of 200 than *C. jejuni* 81-176 (data not shown). The noninvasive *C. jejuni* 81-176 mutant strain RY213 was found at all MOIs to be >100-fold lower in invasion ability (Fig. 1D) than the parental strain (Fig. 1A), as reported previously (64). Thus, *C. jejuni* 81-176 determines its own observed high-efficiency invasion ability.

Saturation kinetic analyses reveal stringent host cell limitation(s) and potential cell cycle dependence for entry. A kinetic analysis over a 2-h invasion period of *C. jejuni* 81-176 entry into INT407 cells was conducted at the above-determined optimal MOI of 200. As shown in Table 1, bacterial invasion was first assessed by an indirect plate count method

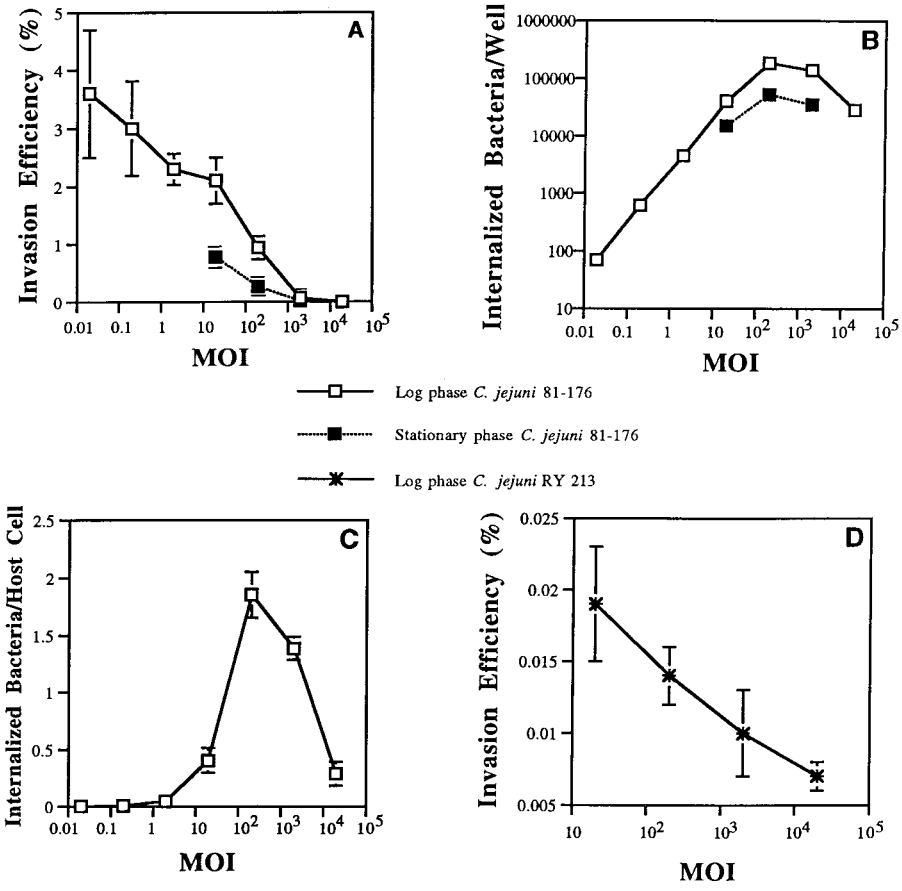

FIG. 1. Comparative kinetic study showing the effect of varying the starting MOI or phase of bacterial growth on *C. jejuni* 81-176 or mutant RY213 invasion efficiency (percentage of the starting inoculum internalized at the end of the assay) versus the number of bacteria internalized into INT407 cells. All assays were conducted in triplicate and repeated on separate days at least three times. (A) Effect of varying the starting MOI and phase of bacterial growth on *C. jejuni* 81-176 invasion efficiency. Invasion assays were conducted, as described in Materials and Methods, by testing a range of starting bacterial concentrations (expressed as MOIs) and using a 2-h invasion period and a 2-h gentamicin kill period prior to enumeration of internalized bacteria. Results are presented as the mean invasion efficiency ± SE. (B) Effect of varying the starting MOI and phase of bacterial growth on total number of bacteria internalized. Invasion assays were conducted as described above. Total number of internalized bacteria per assay well is expressed as CFU per well. Results are presented as the mean CFU per well ± SE. Numbers of CFU per well obtained at MOIs of 200 and 2,000 were significantly greater than numbers of CFU internalized at lower starting MOIs ($P < 0.01$). (C) Effect of varying the MOI on the resulting number of internalized bacteria averaged per epithelial cell. Invasion assays were conducted as described above. The total number of internalized log-phase *C. jejuni* 81-176 bacteria is expressed as the average number of bacteria internalized per epithelial cell (obtained by dividing total internalized bacteria by 10^5 epithelial cells in each well). Results are presented as the mean of the average number of bacteria per epithelial cell ± SE. The resulting averaged numbers of bacteria per epithelial cell at MOIs of 200 or 2,000 were significantly ($P < 0.01$) greater than numbers obtained at lower starting MOIs. (D) Effect of varying the MOI on the invasion efficiency of log-phase *C. jejuni* RY213. Invasion assays were conducted as described for panel A, and results are reported as mean invasion efficiency ± SE.

following a gentamicin kill period. *C. jejuni* entry was easily observed at 10 min, and the total internalized *C. jejuni* increased at each time point up to 2 h. However, the rate of entry was optimal only for the first 90 min and then decreased. When the total number of internalized bacteria, obtained by the indirect plate count method, were averaged over all monolayer cells, the number of bacteria internalized per host cell steadily increased to about 2 (Table 1).

To assess the percentage of INT407 cells infected over time and the actual number of bacteria internalized per infected host cell, we used the AO-CV direct visualization method. The total numbers of stained, live intracellular bacteria observed over time (Table 1) were very similar to those measured by indirect plate count. This direct viewing method revealed that an increasing number of monolayer cells were infected over time. However, after 2 h, only two-thirds of the host cells were infected, with an average of approximately two bacteria per infected host cell. These internalized bacteria were typically observed as well-separated organisms (apparently a result of two separate invasion events).

Extended time course invasion studies in which *C. jejuni* 81-176 was added at an MOI of 20 revealed that an invasion period of 4 h was needed to achieve the same number of internalized bacteria as obtained in 2 h at an MOI of 200 (data not shown). At this 4-h time point, about 70% of the host cells were infected. The number of internalized bacteria reached four per host cell after 7 h of invasion at an MOI of 20, probably due to invasion of some uninfected host cells and mainly to limited intracellular multiplication. Surprisingly, only 85% of monolayer cells were found to be infected after 7 h.

Involvement of MTs and MFs in *C. jejuni* 81-176 invasion. To extend our previous observations (48), we assessed different inhibitors of MT polymerization (colchicine, vinblastine, and vincristine) and used both INT407 and Caco-2 cells to examine the cytoskeletal requirements for invasion into these different human intestinal epithelial cell lines. Compounds that cause

TABLE 1. Kinetic analyses of *C. jejuni* 81-176 entry into INT407 cells[a]

Post-infection time (min)	Indirect viable count assay		Direct visualization AO-CV assay	
	Invasion efficiency (%)	Avg. no. of internalized bacteria/averaged/host cell	% INT407 cells infected	Avg. no. of internalized bacteria/infected host cell
10	0.12 ± 0.04	0.18 ± 0.03	10.33 ± 3.51	1.22 ± 0.00
30	0.67 ± 0.24	0.80 ± 0.17	22.00 ± 3.46	1.85 ± 0.17
60	0.93 ± 0.16	1.13 ± 0.05	51.00 ± 5.57	1.93 ± 0.12
90	1.36 ± 0.17	1.72 ± 0.13	66.33 ± 5.57	2.02 ± 0.18
120	1.42 ± 0.18	1.76 ± 0.29	68.00 ± 3.73	2.13 ± 0.23

[a] Young INT407 cells were infected with *C. jejuni* 81-176 at an MOI of ~200 for various times. The infected host cells were washed with EBSS and incubated for an additional 2 h with fresh medium containing 100 μg of gentamicin per ml; then internalized bacteria were enumerated by indirect bacterial count or observed directly via microscopic analysis of stained, infected monolayers by the AO-CV method as detailed in Materials and Methods. Invasion efficiency represents the percentage of the inoculum internalized by the end of the assay. Total bacteria internalized per well at each time point was divided by 10^5 monolayer cells or the actual number of infected host cells to determine the number of internalized bacteria per host cell or number of internalized bacteria per infected host cell, respectively. The direct visualization method was used to enumerate the actual percentage of host cells containing internalized bacteria. Results shown are the mean ± SE of at least three separate assays.

depolymerization of MFs or MTs were individually used to pretreat INT407 or Caco-2 cell monolayers before and during the 2-h invasion period as described in Materials and Methods. As shown in Fig. 2, regardless of the cell line used cytochalasin D pretreatment resulted in a 95% reduction of the MF-dependent invasion by the control *S. typhi* strain. In contrast, *C. jejuni* 81-176 entry into either cell line was not inhibited by 2 μM cytochalasin D. In fact, MF depolymerization actually stimulated invasion by 81-176 (Fig. 2B), as reported previously (48). When host cells in concomitant studies were pretreated to depolymerize MTs, the entry ability of the control *S. typhi* strain was not reduced. However, the ability of *C. jejuni* 81-176 to invade either INT407 or Caco-2 cells was typically reduced more than 85% by this latter treatment. This inhibition of 81-176 invasion ability by MT depolymerization was inhibitor concentration dependent, as shown in Fig. 2C.

Next we used immunofluorescence microscopy to examine the association of *Campylobacter* with polymerized MTs and MFs at various times during the invasion process. INT407 cells were infected with either *C. jejuni* 81-176 or control *S. typhi* for 30, 60, 120, or 240 min prior to fixation and immunofluorescence analyses as described in Materials and Methods. Initially, bacteria and the host cell MT-based cytoskeleton were differentially labeled with green or red fluorescent tags. Figure 3 shows composite black-and-white representations of fluorescence microscopic images of these *C. jejuni*-infected INT407 cells. Early in infection, bacteria were first observed interacting with the host cell at the tip of a finger-like protrusion of the cell membrane, being extended by one or a few bundled MTs (Fig. 3A). These structures suggest that initiation of invasion involves reorganization of the host cytoskeleton in response to a signal from the adjacent *C. jejuni* since these membrane extensions were not triggered by *S. typhi* in control studies. Next, campylobacters were typically observed during the first 1 to 2 h of the invasion process to be situated in parallel with MT and apparently associated with these structures (Fig. 3B). As shown in Fig. 3C, at 1 h postinfection, representative of the early phases of invasion, bacteria were observed at the periphery of host cells. However, by 4 h postinfection, examination of a number of infected cells revealed that >50% of the observed bacteria had moved intracellularly to a location adjacent to the

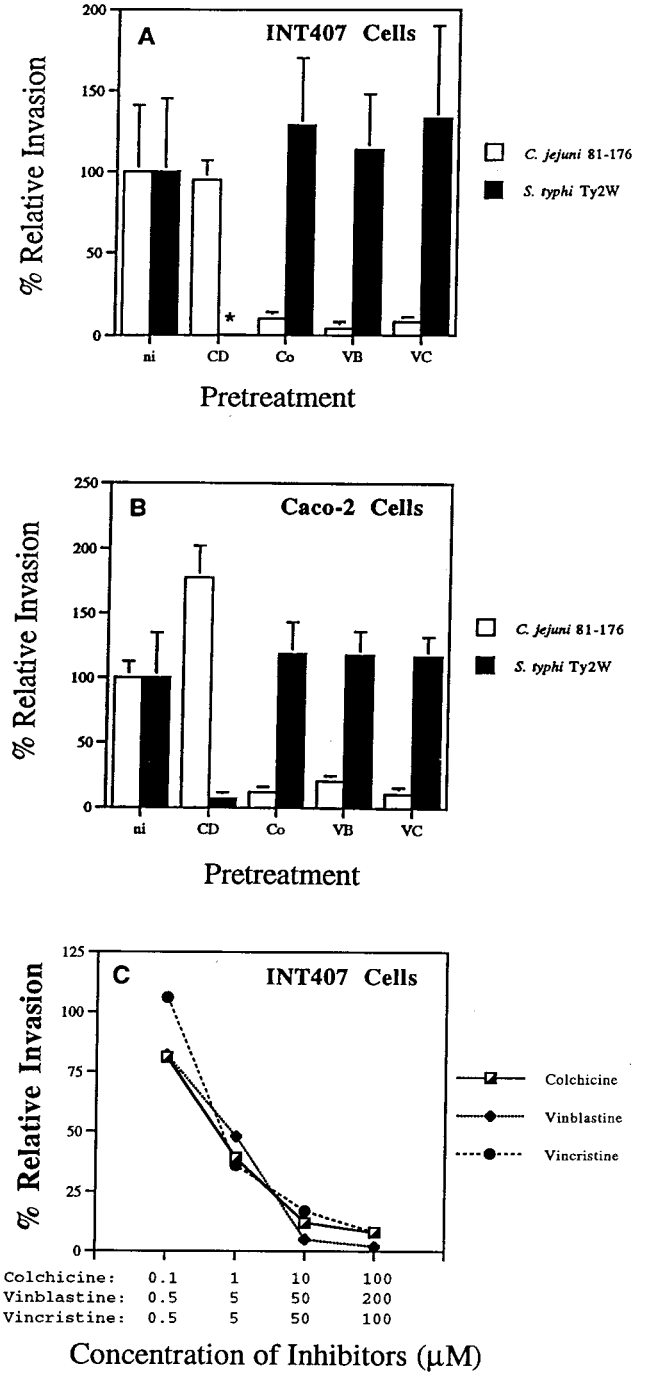

FIG. 2. Effects of various inhibitors on *C. jejuni* 81-176 internalization into INT407 (A) and Caco-2 (B) cells. Data showing the concentration dependence of inhibition are presented in panel C. One hour prior to the addition of bacteria to the monolayer, the epithelial cells were incubated with no inhibitor (ni), with 2 μM cytochalasin D (CD), 10 μM colchicine (Co), 50 μM vinblastine (VB), 50 μM vincristine (VC), or with the various inhibitors at the concentrations listed in panel C. Each inhibitor was maintained throughout the 2-h invasion period. Relative percent invasiveness was determined as recovery in the presence of inhibitors divided by recovery in the absence of inhibitors (i.e., 100% relative invasiveness). *S. typhi* Ty2W served as an MF-dependent invasive control; the asterisk denotes that Ty2W internalization was decreased by >99% in the presence of CD. Results are presented as the mean of at least three separate experiments ± SE, shown as bars above or below the mean.

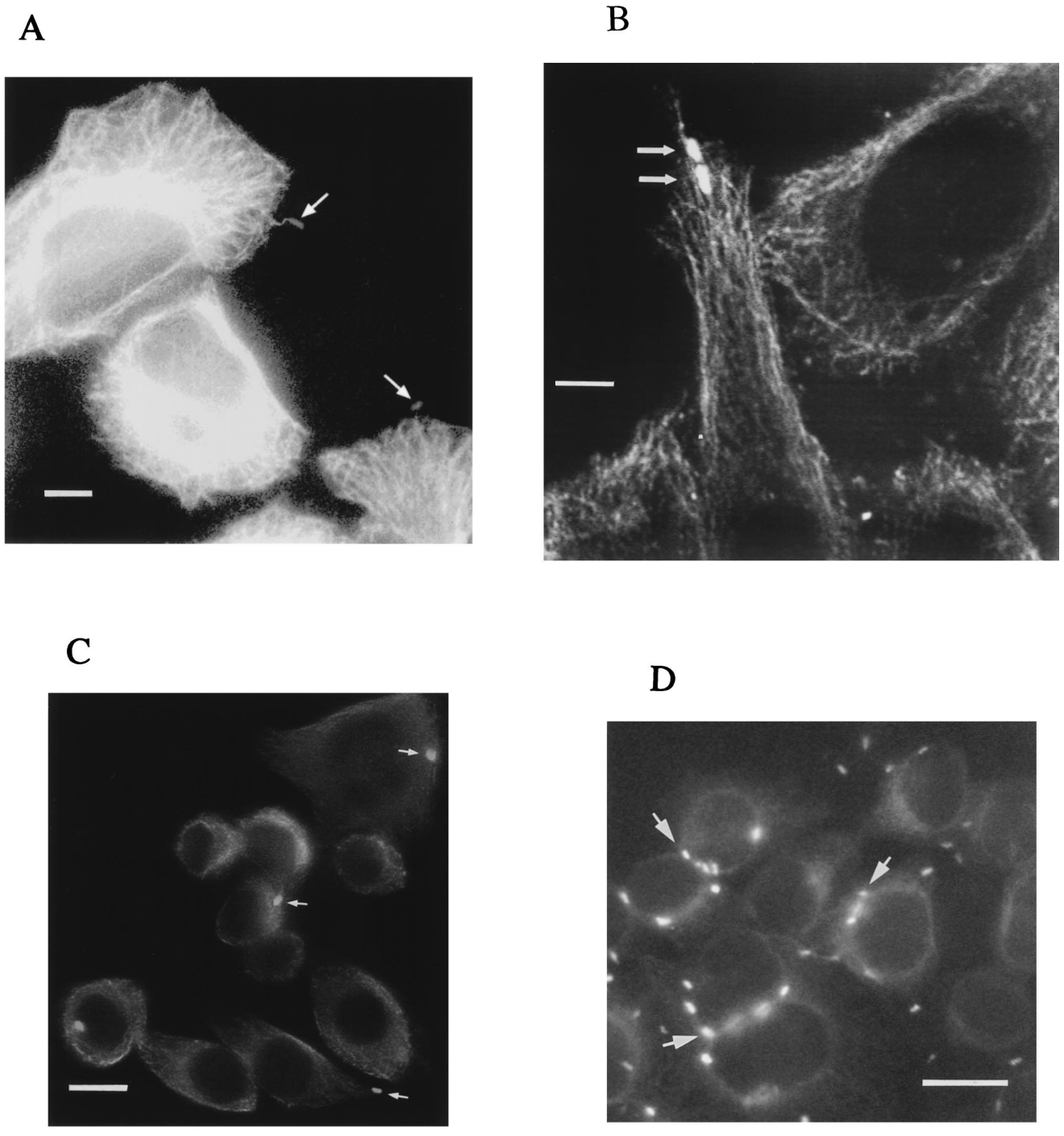

FIG. 3. Representative immunofluorescence microscopic images of *C. jejuni*-infected INT407 cells showing bacterial interactions with MTs over time. INT407 cells infected with *C. jejuni* 81-176 for 1 or 4 h were fixed, permeabilized, and labeled with fluorescent antibodies as described in Materials and Methods. All pixels of light derived from the two different photodetection filters for either the Texas red-X and FITC fluorescent labels have been combined and are shown in white. (A) Fluorescence micrographs of 1-h-infected INT407 cells showing the overall MT-cytoskeleton and MT-based, finger-like membrane protrusions with a single bacterium (arrows) located at the tip of each of two host cell extensions. (B) Confocal fluorescence microscopic image of 1-h-infected INT407 cells. The MTs appear as structural skeletons outlining the cells and the FITC-labeled bacteria (arrows) appear as bright white spots along the MTs. (C) Microscopic image of INT407 cells infected after 1 h, with arrows pointing to bacteria located at the periphery of cells. (D) Immunofluorescence microscopic image of INT407 cells infected for 4 h, with arrows pointing to numerous bacteria located at perinuclear sites within the host cell. Although these stained, infected cell preparations were gently washed with PBS prior to viewing, both intracellular and some extracellular bacteria remain. Bar markers represent 10 μm for (A and B) and 2 μm (C and D).

nucleus (Fig. 3D), similar to a previous report of perinuclear movement of a different *C. jejuni* strain (34). The results of this time course analysis of association of bacteria with MTs indicate that *C. jejuni* initiates contact with the host cell through MT-based, finger-like membrane extensions. The next invasion step seen in this analysis is the association of internalized bacteria in parallel with MTs and movement over 4 h of intracellular bacteria from the cell periphery to the perinuclear

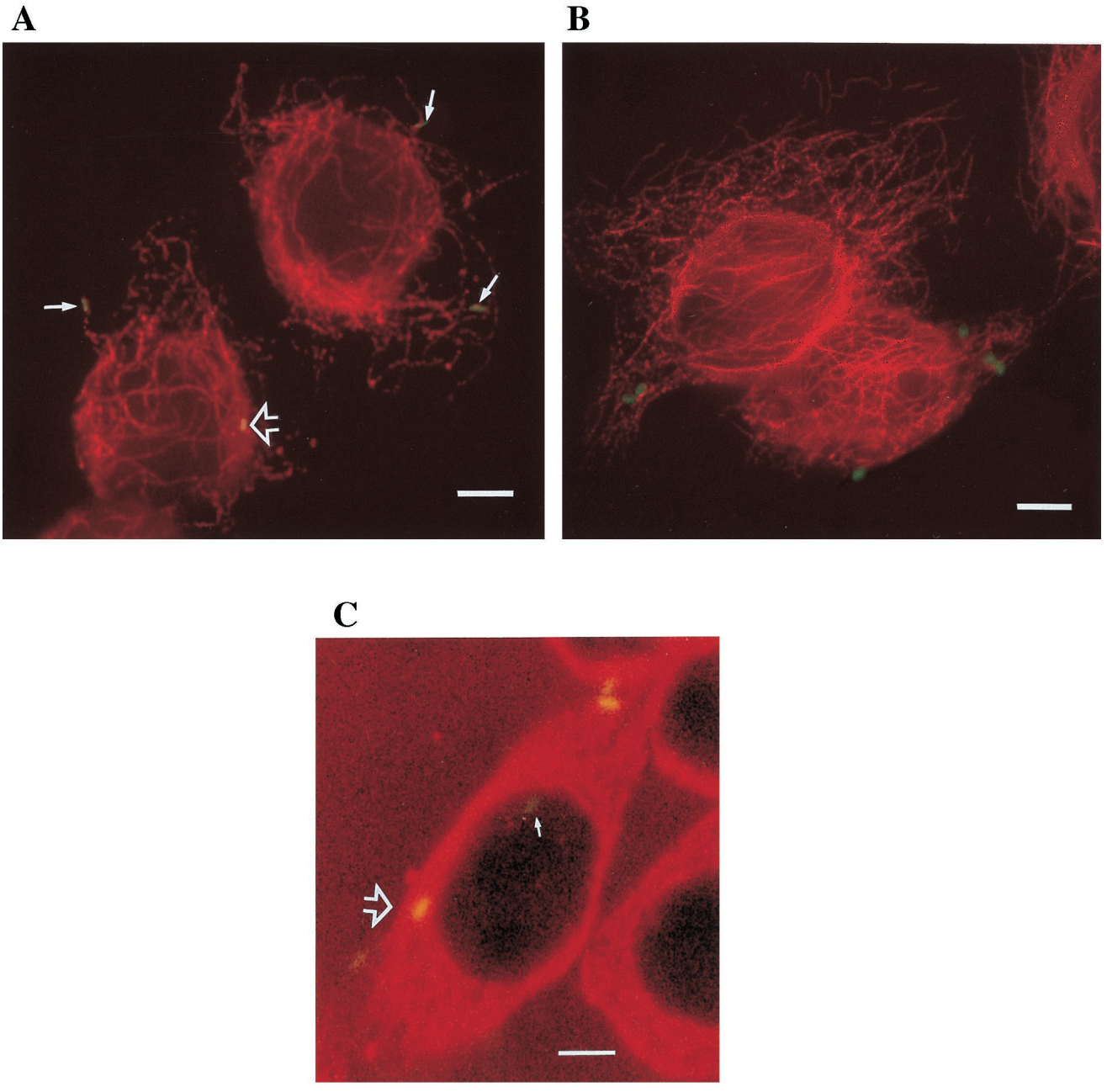

FIG. 4. Representative microscopic images of immunofluorescently labeled *C. jejuni*-infected INT407 cells showing specific colocalization of *C. jejuni* with MT's. Host cells infected with *C. jejuni* 81-176 or control *S. typhi* were prepared and immunolabeled as described in Materials and Methods, using Texas red-X to label MTs and FITC or Oregon Green 514 to label the bacteria. (A) Combined fluorescence image of host cells infected with *C. jejuni* for 1 h, showing bacteria typically aligned with MTs (arrows). Tight colocalization of *C. jejuni* with MTs resulted in a yellow fusion color which could be seen to various degrees with different bacteria (arrowhead). (B) Combined fluorescence image of host cells infected with *S. typhi* for 1 h, showing no apparent specific association of these bacteria with MTs and no color fusion structures. (C) One confocal microscopic laser plane section of 13 total sections of this host cell, showing a faint green non-MT-associated campylobacter (arrow) and one bacterium tightly colocalized with MTs which appears as a yellow fusion color (large arrowhead). Bar markers represent 10 μm.

region. In concomitant studies, neither *C. jejuni* mutant strain RY213 nor *S. typhi* typically exhibited any similar physical orientation with respect to MTs, and no MT-based, finger-like membrane protrusions were seen at the point of host cell contact with these control organisms.

Fluorescence microscopic examination of the association of *C. jejuni* (labeled green) with MTs (labeled red) revealed that most bacteria aligned closely with MTs at 1 to 4 h postinfection, as exemplified in Fig. 4A. At this early stage of infection, some *C. jejuni* could be observed at the tip of finger-like MT extensions of the host cell membrane, some *C. jejuni* were observed to lie in parallel with MTs, and some bacteria formed apparent tight colocalization with MTs which resulted in yellow fusion structures (Fig. 4A). In contrast, concurrent analyses of *S. typhi*-infected monolayers showed no apparent specific association of *S. typhi* with MTs, and no yellow fusion structures indicative of tight colocalization were observed (Fig. 4B). Confocal laser scanning microscopy was used to determine

more accurately whether *C. jejuni* forms a specific and tight association with MTs. The formation of a fusion color between associated structures within a thin laser plane image of a cell is considered a strong molecular indication of colocalization of these two structures. Shown in Fig. 4C, which represents a typical laser plane section (of 13 total sections) of an infected cell, are several bacteria, with evidence of one MT-colocalized bacterium exhibiting a yellow fusion structure. Similar fusion structures were not observed in *S. typhi*-infected host cells by confocal microscopic analysis.

We used similar fluorescence microscopic methods to search for any association of *C. jejuni* 81-176 with polymerized actin (Fig. 5). As reported by others (17, 20), polymerized actin condensation was observed at the point of contact between *Salmonella* spp. and the host cell membrane (Fig. 5C and D). However, host membrane-bound *C. jejuni* 81-176 did not trigger similar actin condensation at the point of host cell contact (Fig. 5A and B). *C. jejuni* 81-176 also did not show evidence of colocalization with MFs at any time points studied. Thus, these immunofluorescence studies (Fig. 4) revealed a tight association of *C. jejuni* with MTs, but not MFs, during the invasion process.

Involvement of dynein in *C. jejuni* 81-176 invasion. Dynein is known to be responsible for MT-dependent, minus-end-directed vesicle transport from the host cell surface to the perinuclear region. We wondered if dynein is required for initial uptake of *C. jejuni* into host cells or is involved subsequently as an MT motor in the molecular trafficking of endosomes containing *C. jejuni* to the perinuclear region. Orthovanadate, a well-described inhibitor of dynein activity (21), was used to ascertain if dynein is required for *C. jejuni* internalization. Figure 6 shows that Na_3VO_4, at a concentration of 100 μM, significantly ($P < 0.01$) reduced the entry of *C. jejuni* 81-176, but not *S. typhi*, into epithelial cells, suggesting a role for dynein in the initial uptake event. In addition, immunofluorescence microscopic studies were conducted to see if *C. jejuni* specifically colocalizes with dynein during the invasion process. At 1 h postinfection, when invading bacteria were shown to colocate with MTs (Fig. 3 and 4), the organisms were also observed to colocalize with dynein (Fig. 7A and B), suggesting a role for dynein in the intracellular molecular trafficking of strain 81-176. In contrast, invading *S. typhi* were not found to collocate with dynein (Fig. 7C and D).

DISCUSSION

Pathogenic microorganisms utilize a variety of different molecular strategies to subvert host cell mechanisms and enable these pathogens to invade susceptible host cells (16, 18, 23, 30, 32, 44). Certain viruses and *Chlamydia psittaci* bind to receptors on the host cell surface and are internalized by the process of receptor-mediated endocytosis (24, 28, 42), which does not require the overt involvement of MTs or MFs. Some pathogens utilize MF-dependent entry processes which mimic phagocytosis (i.e., Fc or C3 receptor-mediated uptake [26]) but utilize different ligands and receptors to zipper the host membrane tightly around the pathogen (e.g., *Chlamydia trachomatis* [5] and the *Yersinia enterocolitica inv* pathway [30, 44]). Some chlamydiae then transit along MTs within the host to the perinuclear region, where pathogen maturation apparently occurs (6). Invasive *Salmonella* or *Shigella* spp. induce a host actin-based cytoskeletal reorganization which leads to MF-dependent macropinocytotic membrane engulfment of these pathogens (7, 17, 18, 23, 29). Somewhat different, *Listeria monocytogenes* recognizes E-cadherin as a receptor and enters host cells via an MF-dependent process (43). Interestingly, once inside a host cell, *L. monocytogenes* (8), *Shigella* (23), *Rickettsia* (27), and vaccinia virus (9) polymerize actin to move within the host cell. In contrast to at least a limited molecular understanding of many of the processes described above, some microorganisms (e.g., *Neisseria gonorrheae* [41, 51], *Citrobacter freundii* [48], and *C. jejuni* VC84 [48]) enter cells via yet largely uncharacterized mechanisms that require MTs and/or MFs. *C. jejuni* isolates have been variously reported to have different host cytoskeletal requirements for invasion, depending on the bacterial strain and host cell used (15, 36, 48). This is akin to the divergent host cell requirements encountered with different serovars of *Chlamydia* (6, 39, 40). The present study was aimed specifically at further characterizing the MT-dependent entry pathway utilized by *C. jejuni* 81-176, a strain that has been used in human feeding experiments (1) and in numerous genetic, biochemical, and vaccine studies (11, 50, 58, 64).

C. jejuni 81-176 enters young, semiconfluent INT407 and Caco-2 cells in a 2-h invasion period with typical invasion efficiencies of 1 to 2%; slightly decreased entry occurs in older confluent monolayers (28a). This level of entry is generally 10^3-fold higher than the level of entry of noninvasive *E. coli* control strains into these host cells. This efficient internalization of wild-type *C. jejuni* 81-176, together with the observation that the RY213 mutant is markedly decreased in invasion ability, indicates that 81-176 is responsible for inducing its novel uptake into host cells. Previous studies have shown that *C. jejuni* motility is required for invasive ability (25, 60, 64), but other invasion-essential genes and functions have not yet been identified. Preliminary electron microscopic (EM) studies previously suggested that these bacteria may propel themselves past the zona occludens, where they are endocytosed basolaterally (37, 48). However, definitive EM analyses of the early steps in the *C. jejuni* invasion process are lacking. The invasion efficiency for *C. jejuni* 81-176 is similar to that observed with the *Yersinia inv* system (30, 31, 32, 44) or *S. typhimurium* (51). However, the reported invasion efficiencies of different *C. jejuni* strains vary widely, from <0.001% (the level of entry of noninvasive *E. coli* HB101) to ~4%, with most strains being very inefficient (57).

Kinetic analyses of strain 81-176 invasion revealed that optimal invasion efficiency (percentage of the inoculum recovered as internalized at the end of the assay) was highest at the lowest MOI (0.02) but that a maximal number of internalized *C. jejuni* was not observed until after infection at an MOI of 200. This finding contrasts sharply with results for *S. typhi*, for example, where the optimal invasion efficiency occurred at an MOI of 40 and the maximal number of internalized bacteria was achieved at MOIs of 40 and above (29). These data suggest that *S. typhi* entry may be a cooperative process involving the accumulation of host cell signaling events to trigger the entry process. The fact that *C. jejuni* 81-176 invasion efficiency was highest at an MOI of 0.02 suggests that this organism is a highly efficient solitary invader at very low bacterial concentrations, as long as it is motile. In contrast, *S. typhi* Ty2W exhibits a much higher maximal invasion efficiency (i.e., 50 to 70%) but only at a 3-log-higher MOI (29). Apparently, some host cell factor(s) limits *S. typhi* internalization to a maximum of 8 to 10 internalized bacteria per host cell regardless of MOI (29). *C. jejuni* invasion, on the other hand, is evidently more tightly regulated by the host, as only two bacteria are maximally internalized per host cell and not all host cells are susceptible to invasion even after 7 h. The visible autoagglutination of 81-176 at increasing cell densities, reported by Misawa and Blaser (46), may reduce motility and be responsible for the steadily decreasing invasion efficiency observed at higher MOIs. Nevertheless, these data suggest that *C. jejuni* 81-176 invasion of

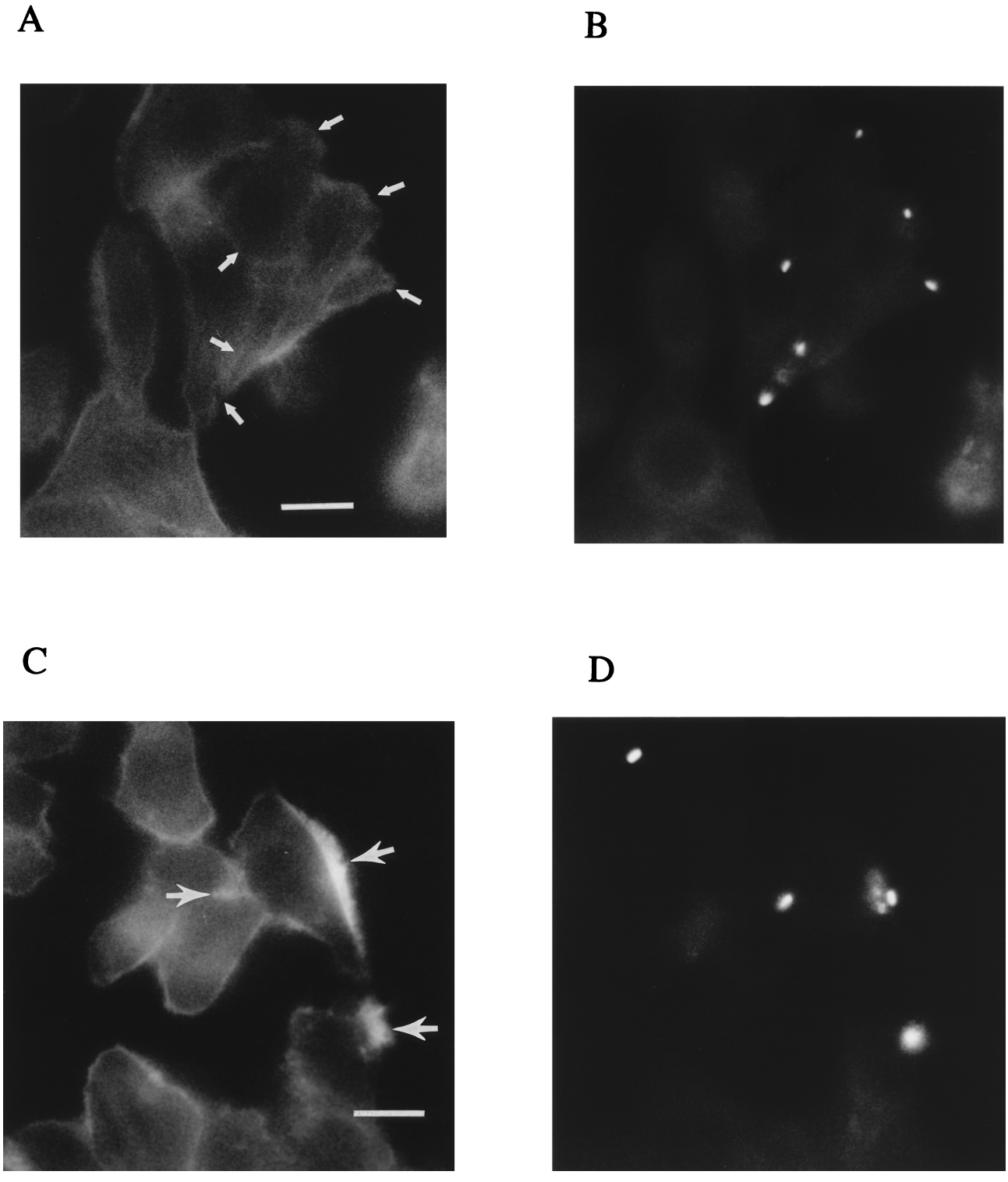

FIG. 5. Representative immunofluorescence microscopic images of *C. jejuni*- and *S. typhi*-infected INT407 cells to examine bacterial association with polymerized actin. Infected host cells were prepared and immunolabeled as described in Materials and Methods, using differential fluorescence labels. In these photomicrographs, all pixels of light derived from the blue photodetector channel (actin; A and C) and green channel (bacteria; B and D) are shown in white. (A) Polymerized actin observed at 30 min postinfection in host cells infected with *C. jejuni*. (B) Corresponding microscopic field showing immunolabeled *C. jejuni*. The positions of bacteria in panel B are indicated in panel A by arrows and are not associated with areas of actin condensation. (C) Polymerized actin observed at 30 min postinfection in host cells infected with *S. typhi*. (D) Corresponding microscopic field showing immunolabeled *S. typhi*. The positions of several bacteria in panel D are indicated in panel C by arrows and are clearly associated with actin condensation. Bar markers represent 2 μm.

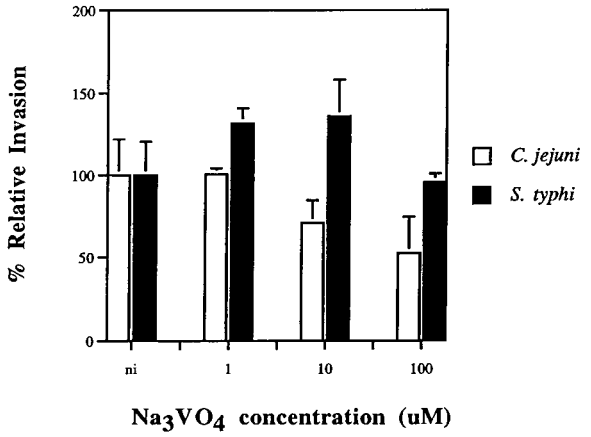

FIG. 6. Effect of inhibition of host cell dynein on *C. jejuni* 81-176 invasion ability. Thirty minutes before bacteria were added to the monolayer, the epithelial cells were incubated either with no inhibitor (ni) or with 1, 10, or 100 μM Na_3VO_4. This dynein inhibitor was maintained throughout the 2-h invasion period. Relative percent invasiveness was determined as recovery in the presence of inhibitors divided by recovery in the absence of inhibitors (i.e., 100% relative invasiveness). *C. jejuni* invasion in the absence of inhibitor was significantly ($P < 0.01$) reduced by monolayer pretreatment with 100 μM Na_3VO_4. *S. typhi* Ty2W served as an invasive control which is not affected by dynein inhibition.

INT407 cells occurs by a highly efficient and kinetically saturable process (reaching maximal internalized bacteria in 2 h at an MOI of 200 or in 4 h at an MOI of 20).

Direct visualization of time course-infected INT407 cells verified the number of internalized bacteria enumerated by indirect viable count. Moreover, this AO staining method showed that after 2 h of infection with strain 81-176 at an MOI of 200, one-third of the monolayer cells remained uninfected. This same high level of uninfected host cells was also apparent after 4 h of infection at an MOI of 200 (data not shown), suggesting that even at high MOIs, some host cells are apparently not susceptible to *C. jejuni* infection. This finding contrasts sharply with invasion of 100% of INT407 cells within 30 min to 1 h by *S. typhi*, depending on the starting MOI (29). Since the percentage of *C. jejuni*-infected host cells gradually increases with time and about 85% of monolayer cells become infected after a 7-h invasion period, it appears that *C. jejuni* entry may be host cell cycle dependent. Recently, the cytolethal distending toxin of *C. jejuni* has been reported to lock cells in cell cycle phase G_2 (62) and may play a role in susceptibility of host cells to *C. jejuni*.

Optimally infected host cells contained two well-separated *C. jejuni* organisms per infected cell, suggesting that these bacteria were engulfed in different uptake events. Increasing the invasion period to 7 h increased total number of internalized bacteria ~2-fold, probably due mainly to limited intracellular replication. Thus, *C. jejuni* 81-176 internalization occurs by a process that strictly limits the number of bacteria taken up per cell (to about two per cell) and in which the infected host cells become saturated for entry, even at higher MOIs or over longer periods of time. This tight restriction on entry may reflect a limited number of host cell invasion receptor or entry sites, a limitation of some other host biochemical requisite for entry, and/or host cell modifications occurring during invasion that prevent further *C. jejuni* entry. Finally, the invasion ability of *C. jejuni* 81-176 grown to early stationary phase (OD_{600} of ~1.2) was only three- to fivefold lower than that of mid-log-phase bacteria. The requirement for de novo bacterial protein synthesis for *C. jejuni* invasion (34, 48) may partially explain the reduced invasion levels observed with stationary-phase bacteria.

C. jejuni 81-176 enters INT407 cells via a novel mechanism that requires host cell MTs but not MFs (48). This requirement was shown to be inhibitor concentration dependent and was extended to Caco-2 cells in controlled studies here, demonstrating that this *C. jejuni* invasion process is not unique to INT407 cells. This cytoskeletal requirement for strain 81-176 invasion is readily reproducible in our assays but differs from that reported by Russell et al. (55), possibly due to methodological differences. Strain 81-176 is not unique among *Campylobacter* spp. in its strong involvement of MTs during entry. Invasion by *C. coli* VC167 (48a) and other strains of *C. jejuni* (28a) also show an MF-independent requirement for polymerized MTs. Nevertheless, reports of differing invasion requirements for other *C. jejuni* strains (33, 35, 48) make it likely that different *Campylobacter* strains, similar to different *Chlamydia* serovars, use different mechanisms for cell invasion. The previously reported change in cytoskeletal requirements for invasion by *Citrobacter* strains, depending on the specific host cell line used, suggests that some bacteria may encode several invasion mechanisms, each of which requires certain host receptors or other host factors which are not expressed by all cell types (i.e., tissue tropism).

The immunofluorescence microscopic imaging data provided herein demonstrate tight colocalization of 81-176 cells with MTs during invasion, similar to observations reported recently for *Chlamydia* (6). Although *C. jejuni* 81-176 colocalizes with MTs, tubulin does not accumulate massively at the point of bacterium-host cell contact. Control *S. typhi* did not colocalize with MTs during entry but, in marked contrast to 81-176, showed a notable accumulation of F-actin at the site of bacterial contact with the host cell as reported earlier for *Salmonella* (18).

These fluorescence microscopic analyses of *C. jejuni* invasion reveal the temporal interaction of strain 81-176 with various host cell structures and allow us to propose a coherent invasion mechanism. At early times during invasion, *C. jejuni* organisms are observed interacting with finger-like extensions of the cell membrane containing one or a few bundled MTs. It is important to note that these thin, MT-based membrane extensions were frequently observed during the first hour of invasion but required dense immunostaining of MTs for observation of these slender structures. Possibly these membrane extensions represent an early host cell cytoskeletal response to a diffusible signal from the nearby bacterium. Konkel et al. previously reported that *C. jejuni* synthesizes novel proteins upon contact with host cells (37). Initial internalization of 81-176 requires polymerized MTs, but is not inhibited by stabilizing MTs with taxol, a feature that distinguishes this MT-dependent uptake mechanism from that of *Citrobacter freundii* (48). Inhibitors affecting the formation of host membrane invaginations also block the internalization of *C. jejuni* (33, 48, 63), suggesting that the host cell invasion receptor may reside in related structures. Internalized *Campylobacter* are colocalized both with MTs and dynein during the infection process. Also, limited EM studies of internalized *C. jejuni* have previously shown that these bacteria are contained intracellularly within membrane-bound vacuoles (34, 48, 56). Orthovanadate, an inhibitor of dynein-mediated vesicle trafficking, was found to reduce entry significantly. These findings indicate that dynein may play a role in both *C. jejuni* initial entry and movement intracellularly along MTs. We hypothesize from these findings that a successful *Campylobacter* ligand-host cell receptor interaction might activate dynein bound in caveolae within the host cell membrane and cause this activated dynein to transverse inwardly along a MT and consequently invaginate the dynein-bound membrane, resulting in engulfment of the

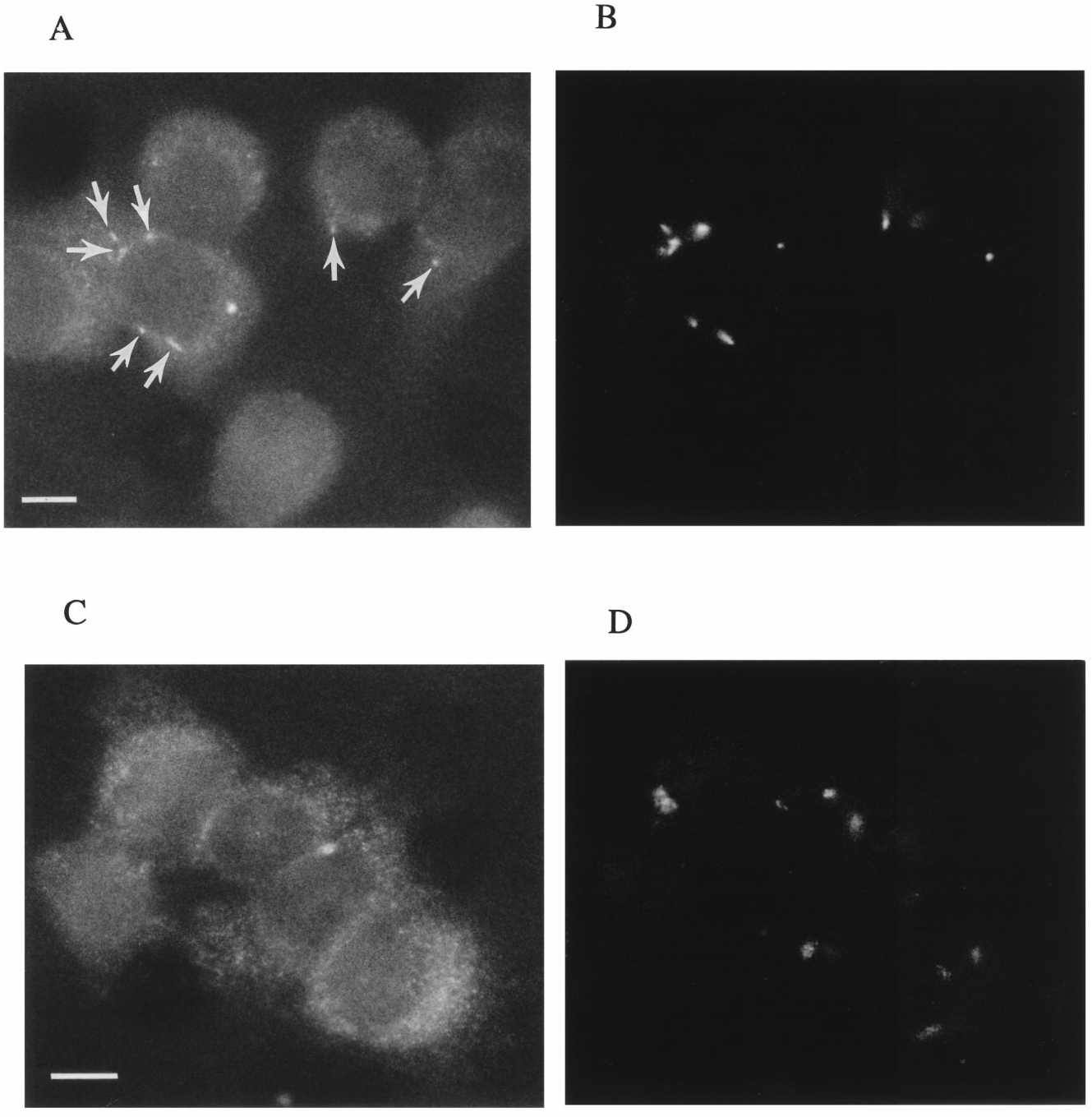

FIG. 7. Representative immunofluorescence microscopic images of *C. jejuni*- and *S. typhi*-infected INT407 cells to examine bacterial association with dynein. Infected host cells were prepared and immunolabeled as described in Materials and Methods, using differential fluorescence labels. In these photomicrographs, all pixels of light derived from Texas red-X (dynein; A and C) and FITC (bacteria; B and D) are shown in white. (A) Dynein observed in host cells infected with *C. jejuni* for 1 h. (B) Corresponding microscopic field showing immunolabeled *C. jejuni*. The positions of several bacteria in panel B are indicated in panel A by arrows and demonstrate *C. jejuni* colocalization with dynein. (C) Host cell dynein observed after 1 h of infection with *S. typhi*. (D) Corresponding microscopic field showing immunolabeled *S. typhi*. Invading *S. typhi* did not colocate with dynein. Bar markers represent 1 μm.

adjacent bound external bacterium. Trafficking of the endosome-contained *C. jejuni* from the cell surface to the perinuclear region would, accordingly, involve the MT molecular motor dynein. Finally, recent evidence has revealed that MTs are associated at the host plasma membrane with the APC protein (47, 52). In preliminary experiments, monolayer pretreatment with monoclonal antibody that recognizes a surface-exposed region of APC did not reduce *C. jejuni* internalization, failing to implicate APC as a major host cell receptor for *C. jejuni* invasion (28a).

Together, these results have provided a framework of kinetic data and structural interactions from which initial inferences about the 81-176 invasion mechanism have been derived. These data show that *C. jejuni* 81-176 triggers an efficient and kinetically saturable invasion of intestinal epithelial cells. The invasion mechanism is dependent on host cell MTs and may

involve the trafficking of *C. jejuni* within endosomes, via the MT motor dynein, along the MTs to designated sites (i.e., perinuclear region) within the cell. The pathophysiological mechanism(s) which *C. jejuni* utilizes to cause diarrheal or dysenteric syndromes remains uncharacterized. Improved understanding of the molecular mechanism of *C. jejuni* invasion and intracellular movement should aid both our perception of disease pathogenesis and the development of new chemotherapeutic and prophylactic methods.

ACKNOWLEDGMENTS

We are grateful to P. Guerry-Kopecko and X.-Z. Huang for strains, antibodies, and helpful technical advice. We thank L. Harvath (FDA-CBER, Bethesda, Md.) and M. Adelman and T. A. Baginski (Biomedical Instrumentation Center, USUHS, Bethesda, Md.) for assistance with the confocal microscopy, and we thank C. Deal, M. Alavi, M. Schmidt, and P. Guerry-Kopecko for critical review of the manuscript.

Lan Hu was supported by a fellowship from the Fogarty International Center at NIH.

REFERENCES

1. **Black, R. E., M. M. Levine, M. L. Clements, T. P. Hughes, and M. J. Blaser.** 1988. Experimental *Campylobacter jejuni* infection in humans. J. Infect. Dis. **157:**472–479.
2. **Blaser, M. J., I. D. Berkowitz, F. M. Laforce, J. Cravens, L. B. Reller, and W. L. Wang.** 1979. *Campylobacter* enteritis: clinical and epidemiologic features. Ann. Intern. Med. **91:**179–185.
3. **Blaser, M. J., B. M. Allos, and D. Lang.** 1997. Development of Guillain-Barré syndrome following *Campylobacter* infection. J. Infect. Dis. **176**(Suppl. 2)**:**S91.
4. **Blaser, M. J., J. G., Wells, R. A. Feldman, R. A. Pollard, and J. R. Allen.** 1983. *Campylobacter* enteritis in the United States. A multicenter study. Ann. Intern. Med. **98:**360–365.
5. **Byrne, G. I., and J. W. Moulder.** 1978. Parasite-specified phagocytosis of *Chlamydia psittaci* and *Chlamydia trachomatis* by L and HeLa cells. Infect. Immun. **19:**598–606.
6. **Clausen, J. D., G. Christiansen, H. U. Holst, and S. Birkelund.** 1997. *Chlamydia trachomatis* utilizes the host cell microtubule network during early events of infection. Mol. Microbiol. **25:**441–449.
7. **Clerc, P., and P. J. Sansonetti.** 1987. Entry of *Shigella flexneri* into HeLa cells: evidence for directed phagocytosis involving actin polymerization and myosin accumulation. Infect. Immun. **55:**2681–2688.
8. **Cossart, P., and C. Kocks.** 1994. The actin-based motility of the facultative intracellular pathogen *Listeria monocytogenes*. Mol. Microbiol. **13:**395–402.
9. **Cudmore, S., P. Cossart, G. Griffiths, and M. Way.** 1995. Actin-based motility of vaccinia virus. Nature **378:**636–638.
10. **De Melo, M. A., G. Gabbiani, and J. C. Pechere.** 1989. Cellular events and intracellular survival of *Campylobacter jejuni* during infection of HEp-2 cells. Infect. Immun. **57:**2214–2222.
11. **Doig, P., R. Yao, D. H. Burr, P. Guerry, and T. J. Trust.** 1996. An environmentally regulated pilus-like appendage involved in *Campylobacter* pathogenesis. Mol. Microbiol. **20:**885–894.
12. **Duffy, M. C., J. B., Benson, and S. J. Rubin.** 1980. Mucosal invasion in *Campylobacter* enteritis. Am. J. Clin. Pathol. **73:**706–708.
13. **Elsinghorst, E. A.** 1994. Measurement of invasion by gentamicin resistance. Methods Enzymol. **236:**405–420.
14. **Elsinghorst, E. A., L. S. Baron, and D. J. Kopecko.** 1989. Penetration of human intestinal epithelial cells by *Salmonella*: molecular cloning and expression of *Salmonella typhi* invasion determinants in *Escherichia coli*. Proc. Natl. Acad. Sci. USA **86:**5173–5177.
15. **Fauchere, J. L., A. Posenau, M. Veron, E. N. Moyen, S. Richard, and A. Pfister.** 1986. Association with HeLa cells of *Campylobacter jejuni* and *Campylobacter coli* isolated from human feces. Infect. Immun. **54:**283–287.
16. **Falkow, S., R. R. Isberg, and D. A. Portnoy.** 1992. The interaction of bacteria with mammalian cells. Annu. Rev. Cell Biol. **8:**333–363.
17. **Finlay, B. B., and S. Falkow.** 1988. Comparison of the invasion strategies use by *Salmonella cholerae-suis*, *Shigella flexneri* and *Yersinia enterocolitica* to enter cultured animal cells; endosome acidification is not required for bacterial invasion or intracellular replication. Biochimie **70:**1089–1099.
18. **Finlay, B. B., and S. Falkow.** 1989. Common themes in microbial pathogenicity. Microbiol. Rev. **53:**210–230.
19. **Finlay, B. B., J. Fry, E. P. Rock, and S. Falkow.** 1989. Passage of *Salmonella* through polarized epithelial cells; role of the host and bacterium. J. Cell Sci. Suppl. **11:**99–107.
20. **Finlay, B. B., and S. Falkow.** 1990. *Salmonella* interactions with polarized human intestinal Caco-2 epithelial cells. J. Cell Sci. **162:**1096–1106.
21. **Finlay, B. B., S. Ruschkowski, and S. Dedhar.** 1991. Cytoskeletal rearrangements accompanying *Salmonella* entry into epithelial cells. J. Cell Sci. **99:** 283–296.
22. **Gibbons, I. R., M. P. Cosson, J. A. Evans, B. H. Gibbons, B. Houck, K. H. Martinson, W. S. Sale, and W. J. Tang.** 1978. Potent inhibition of dynein adenosinetriphosphatase and of the motility of cilia and sperm flagella by vanadate. Proc. Natl. Acad. Sci. USA **75:**2220–2224.
23. **Goldberg, M. B., and P. J. Sansonetti.** 1993. *Shigella* subversion of the cellular cytoskeleton: a strategy for epithelial colonization. Infect. Immun. **61:**4941–4946.
24. **Goldstein, J. L., R. G. Anderson, and M. S. Brown.** 1979. Coated pits, coated vesicles and receptor-mediated endocytosis. Nature **279:**679–685.
25. **Grant, C. C., M. E. Konkel, W. Cieplak, Jr., and L. S. Tompkins.** 1993. Role of flagella in adherence, internalization, and translocation of *Campylobacter jejuni* in nonpolarized and polarized epithelial cell cultures. Infect. Immun. **61:**1764–1771.
26. **Griffin, F. M., Jr., J. A. Griffin, and S. C. Silverstein.** 1976. Studies on the mechanism of phagocytosis. II. The interaction of macrophages with anti-immunoglobulin IgG-coated bone marrow-derived lymphocytes. J. Exp. Med. **144:**788–809.
27. **Heinzen, R. A., S. F. Hayes, M. G. Peacock, and T. Hackstadt.** 1993. Directional actin polymerization associated with spotted fever group *Rickettsia* infection of Vero cells. Infect. Immun. **61:**1926–1935.
28. **Helenius, A., J. Kartenbeck, K. Simmons, and E. Fries.** 1980. On the entry of Semliki forest virus into BHK-21 cells. J. Cell Biol. **84:**404–420.

28a. **Hu, L., and D. Kopecko.** Unpublished data.

29. **Huang, X.-Z., B. Tall, W. Schwan, and D. J. Kopecko.** 1998. Physical limits on *Salmonella typhi* entry into cultured human intestinal epithelial cells. Infect. Immun. **66:**2928–2937.
30. **Isberg, R. R., and S. Falkow.** 1985. A single genetic locus encoded by *Yersinia pseudotuberculosis* permits invasion of cultured animal cells by *Escherichia coli* K-12. Nature **317:**262–264.
31. **Isberg, R. R., and G. T. Van Nhieu.** 1994. Two mammalian cell internalization strategies used by pathogenic bacteria. Annu. Rev. Genet. **28:**395–422.
32. **Isberg, R. R., D. L. Voorhis, and S. Falkow.** 1987. Identification of invasin: a protein that allows enteric bacteria to penetrate cultured mammalian cells. Cell **50:**769–778.
33. **Ketley, J. M.** 1997. Pathogenesis of enteric infection by *Campylobacter*. Microbiology **143:**5–21.
34. **Konkel, M. E., and W. Cieplak, Jr.** 1992. Altered synthetic response of *Campylobacter jejuni* to cocultivation with human epithelial cells is associated with enhanced internalization. Infect. Immun. **60:**4945–4949.
35. **Konkel, M. E., S. F. Hayes, L. A. Joens, and W. Cieplak, Jr.** 1992. Characteristics of the internalization and intracellular survival of *Campylobacter jejuni* in human epithelial cell cultures. Microb. Pathog. **13:**357–370.
36. **Konkel, M. E., and L. A. Joens.** 1989. Adhesion to and invasion of HEp-2 cells by *Campylobacter* spp. Infect. Immun. **57:**2984–2990.
37. **Konkel, M. E., D. J. Mead, S. F. Hayes, and W. Cieplak, Jr.** 1992. Translocation of *Campylobacter jejuni* across human polarized epithelial cell monolayer cultures. J. Infect. Dis. **166:**308–315.
38. **Korlath, J. A., M. T. Osterholm, L. A. Judy, J. C. Forfang, and R. A. Robinson.** 1985. A point-source outbreak of campylobacteriosis associated with consumption of raw milk. J. Infect. Dis. **152:**592–596.
39. **Majeed, M., and E. Kihlstrom.** 1991. Mobilization of F-actin and clathrin during redistribution of *Chlamydia trachomatis* to an intracellular site in eucaryotic cells. Infect. Immun. **59:**4465–4472.
40. **Majeed, M., M. Gustafasson, E. Kihlstrom, and O. Stendahl.** 1993. Roles of Ca^{2+} and F-actin in intracellular aggregation of *Chlamydia trachomatis* in eucaryotic cells. Infect. Immun. **61:**1406–1414.
41. **Makino, S., J. P. Van Putten, and T. F. Meyer.** 1991. Phase variation of the opacity outer membrane protein controls invasion by *Neisseria gonorrhoeae* into human epithelial cells. EMBO J. **10:**1307–1315.
42. **Matlin, K. S., H. Reggio, A. Helenius, and K. Simmons.** 1981. Infectious entry pathway of influenza virus in a canine kidney cell line. J. Cell Biol. **91:**601–613.
43. **Mengaud, J., H. Ohayon, P. Gounon, R.-M. Mege, and P. Cossart.** 1996. E-cadherin is the receptor for internalin, a surface protein required for entry of *L. monocytogenes* into epithelial cells. Cell **84:**923–932.
44. **Miller, V. L., and S. Falkow.** 1988. Evidence for two genetic loci in *Yersinia enterocolitica* that can promote invasion of epithelial cells. Infect. Immun. **56:**1242–1248.
45. **Millotis, M. D.** 1991. Acridine orange stain for determining intracellular enteropathogens in HeLa cells. J. Clin. Microbiol. **29:**830–831.
46. **Misawa, N., and M. J. Blaser.** 1997. Detection of autoagglutination activity from *Campylobacter jejuni* as a virulence marker, abstr. B-518, p. 117. *In* Abstracts of the 97th General Meeting of American Society for Microbiology 1997. The American Society for Microbiology, Washington, D.C.
47. **Nathke, I. S., C. L. Adams, P. Polakis, J. H. Sellin, and W. J. Nelson.** 1996. The adenomatous polyposis coli tumor suppressor protein localizes to plasma membrane sites involved in active cell migration. J. Cell Biol. **134:** 165–179.
48. **Oelschlaeger, T. A., P. Guerry, and D. J. Kopecko.** 1993. Unusual microtubule-dependent endocytosis mechanisms triggered by *Campylobacter jejuni*

and *Citrobacter freundii*. Proc. Natl. Acad. Sci. USA **90:**6884–6888.
48a. **Oelschlaeger, T. A., P. Guerry, and D. Kopecko.** Unpublished data.
49. **Osborn, M., and K. Weber.** 1982. Immunofluorescence and immunocytochemical procedures with affinity purified antibodies: tubulin containing structures. Methods Cell Biol. **24:**97–132.
50. **Pei, Z., C. Burucoa, B. Grignon, S. Baqar, X.-Z. Huang, D. J. Kopecko, A. L. Bourgeois, J. L. Fauchere, and M. J. Blaser.** 1998. Mutation in the *peb*1A locus of *Campylobacter jejuni* reduces interactions with epithelial cells and intestinal colonization of mice. Infect. Immun. **66:**938–943.
51. **Penheiter, K. L., N. Mathur, D. Giles, T. Fahlen, and B. D. Jones.** 1997. Non-invasive *Salmonella typhimurium* mutants are avirulent because of an inability to enter and destroy M cells of ileal Peyer's patches. Mol. Microbiol. **24:**697–709.
52. **Polakis, P.** 1995. Mutations in the APC gene and their implications for protein structure and function. Curr. Opin. Genet. Dev. **5:**66–71.
53. **Richardson, W. P., and J. C. Sadoff.** 1988. Induced engulfment of *Neisseria gonorrhoeae* by tissue culture cells. Infect. Immun. **56:**2512–2514.
54. **Robinson, D. A.** 1981. Infective dose of *Campylobacter jejuni* in milk. Br. Med. J. (Clin. Res. Ed.). **282:**1584.
55. **Russell, R. G., and D. C. Blake, Jr.** 1994. Cell association and invasion of Caco-2 cells by *Campylobacter jejuni*. Infect. Immun. **62:**3773–3779.
56. **Russell, R. G., M. O'Donnoghue, D. C. Blake, Jr., J. Zulty, and L. J. DeTolla.** 1993. Early colonic damage and invasion of *Campylobacter jejuni* in experimentally challenged infant *Macaca mulatta*. J. Infect. Dis. **168:**210–215.
57. **Schwartz, D., R. Perry, D. M. Dombroski, J. M. Merrick, and J. Goldhar.** 1996. Invasive ability of *C. jejuni*/*coli* isolated from children with diarrhea and the effect of iron-regulated proteins. Zentrbl. Bakteriol. **283:**485–491.
58. **Scott, D. A.** 1997. Vaccines against *Campylobacter jejuni*. J. Infect. Dis. **176**(Suppl. 2)**:**S183–S188.
59. **Skirrow, M. B., and M. J. Blaser.** 1992. Clinical and epidemiological considerations, p. 3–8. *In* I. Nachamkin, M. J. Blaser, and L. S. Tompkins (ed.), *Campylobacter jejuni*: current status and future trends. American Society for Microbiology, Washington, D.C.
60. **Skirrow, M. B., D. M. Jones, E. Sutcliffe, and J. Benjamin.** 1993. *Campylobacter* bacteraemia in England and Wales, 1981–91. Epidemiol. Infect. **110:**567–573.
61. **Wassenaar, T. M., B. A. M. van der Zeijst, R. Ayling, and D. G. Newell.** 1993. Colonization of chicks by motility mutants of *Campylobacter jejuni* demonstrates the importance of flagellin A expression. J. Gen. Microbiol. **139:**1171–1175.
62. **Whitehouse, C. A., P. B. Balbo, E. C. Pesci, D. L. Cottle, P. M. Mirabito, and C. L. Pickett.** 1998. *Campylobacter jejuni* cytolethal distending toxin causes a G_2-phase cell cycle block. Infect. Immun. **66:**1934–1940.
63. **Wooldridge, K. G., P. H. Williams, and J. M. Ketley.** 1996. Host signal transduction and endocytosis of *Campylobacter jejuni*. Microb. Pathog. **21:**299–305.
64. **Yao, R., D. H. Burr, and P. Guerry.** 1997. CheY-mediated modulation of *Campylobacter jejuni* virulence. Mol. Microbiol. **23:**1021–1031.

Editor: V. A. Fischetti